IIW Documents

Techniques For Examining Transformation Behaviour in Weld Metal And HAZ. A STATE OF THE ART REVIEW

- *By O.M. Akselsen, T. Simonsen (Norway)*

Introduction

Transformation behaviour in metals and alloys has been a subject for research for many decades. As problems connected to welding of steels became more obvious (cold cracking and brittle fracture), research programmes were initiated to study the hardenability and transformation behaviour of both the heat affected zone (HAZ) and the weld metal.

The phase transformation that occurs during the welding process is of major importance in determining the metallurgical (and mechanical) properties of both the weld metal and the heat affected zone in a welded joint. Techniques employed for examining transformation behaviour in weldable steels have been developed and improved throughout the years, and the aim of the present review is to summarize recent publications in this field.

1. Phase transformation in HAZ and weld metal

During the last years efforts have been made to produce a quantitative description of weld metal microstructures [1-4]. No similar work has been done for the heat affected zone.

In general, at very rapid cooling rates (low heat input), a massive transformation occurs, resulting in martensite ; the degree of autotempering depends on the Ms-temperature. At slower cooling rates (medium heat input) ferritic components, which are identified either as acicular ferrite (AF) or sideplate structures (AC),* occur. The latter constituent consists of parallel ferrite sideplates with either aligned or , non-aligned martensite-austenite-carbides. A further drop in cooling rate results in parallel plates separated by pearlite or pearlitic carbides, often termed Widmanstattenferrite (WF). In some cases a distinction is made between the coarser microstructures, for instance coarse acicular ferrite (CAF) or lath ferrite (LF) [5]. At the slowest cooling rate (high heat input), the austenite decomposes to proeutectoid ferrite (polygonal or equiaxed ferrite (F) and ferrite-carbide aggregates (FC).

During phase transformation of the fcc to the bcc lattice, the free energy is reduced. The enthalpy difference liberated as heat, ΔH_{trans}, results in a slower cooling rate through the transformation range. This is the basic principle for the thermal analysis method employed in establishing CCT-diagrams.

The change from fcc to bcc crystal lattice and vice versa involves a rearrangement of atoms which results in lattice parameter changes. The volume expansion or contraction is recorded by dilatometric methods.

* The index AC is a matter for some controversy : the ferrite sideplate structures have also been abbreviated FSP [4,5].

Doc. IIS/IIW-894-86 (ex doc. IX-1451-86) prepared on behalf of Commission IX "Behaviour of metals subjected to welding" of the IIW, but not committing the IIW as a whole. Messrs. Akselsen and Simonsen are members of the Norwegian delegation to the IIW.

2. Methods for examining phase transformation

Numerous laboratory techniques have been developed to study phase transformation. Although the A_{c1} and A_{c3} temperatures are of interest, the present discussion is only concerned with phase transformation during the cooling stage. The decomposition of austenite is recorded either by thermal analysis [6-10], dilatometry [6,7,11,12] or magnetic analysis [13]. However, the latter method seems to be of limited use and will not be considered in this review. Furthermore, only thermal analysis and dilatometry techniques have been applied to in situ studies. The following discussion is thus divided into two sections, the weld thermal simulation ("analytical" methods) and the actual welding situation (direct or in situ methods).

2.1 Weld thermal simulation :

The weld thermal simulation technique for reproducing HAZ microstructures, first developed by Nippes and Savage [14], has been

accepted as a convenient method of examining the properties of HAZ regions using small-scale laboratory test specimens. The thermal cycles are similar to those experienced by a particular point in a real HAZ during welding. The specimens are resistance or induction heated, and the dimensions are usually restricted to 11 x 11 mm cross section. Chromel-alumel thermocouples are spot welded at the specimen surface at mid-length, spaced at a separate distance of about 3 to 5 mm between the two wires along the transverse direction. With this type of thermocouple the peak temperature is restricted to an upper level of 1390°C. If higher peak temperatures are desirable, the platinum-platinum/rhodium type should be applied. The lateral expansion or contraction across the specimen at mid-length is very often continuously recorded during the weld thermal simulation cycle. An example of the temperature-time cycle is given below with the corresponding dilatation curve (Fig. 1).

The example in Fig.1 illustrate two transformation points, the start and end of transformation. Using the dilatometry technique, it should be possible to resolve the martensite, bainite and ferrite transformation, with the restriction that a certain amount of the different microstructural components is required for recording.

The thermal analysis method has been successfully used for examining the transformation behaviour. This method has been divided into several groups according to the processing of the signal. Temperature-time, direct rate, differential and derived logarithmic derivation methods have been applied [7,15,16]. An example of employing the simulation technique using a small tubular specimen induction heated in an inert gas atmosphere is illustrated in Fig.2. The heating rate from room temperature up to 1350°C is in the range of 3 to 7 sec and the desired cooling programmes are obtained by gas-cooling.

Temperature-time method : The decomposition of austenite involves heat liberation, which results in a reduction of the cooling rate. The temperature at which this delayed cooling occurs is considered as the start of transformation (T_s). After the end of transformation (T_f), the temperature-time curve approaches its normal curvature, now with a displacement Δt along the time axis (Fig.1). A precise location of both the start and end of transformation is rather difficult using the temperature-time curve. However, by the direct rate analysis method [7] a more exact temperature for start of transformation can be defined.

Successive equal intervals ΔT of temperature are plotted against the temperature resulting

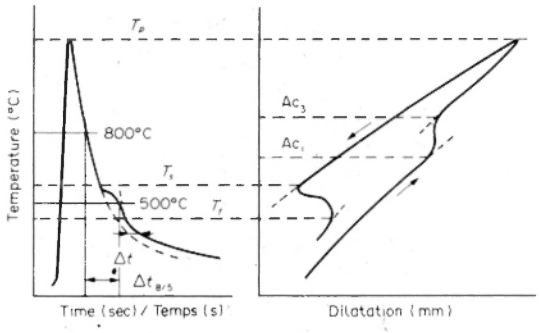

Fig.1 : Schematical illustration of a cooling curve (left) with the corresponding dilatation curve (right).

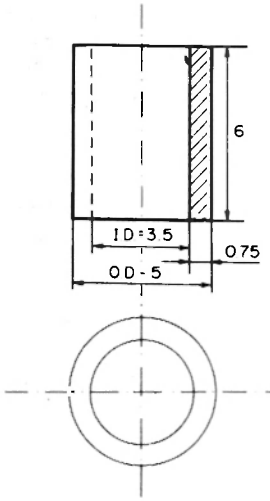

Fig.2 : Example of specimen geometry and dimensions (mm).

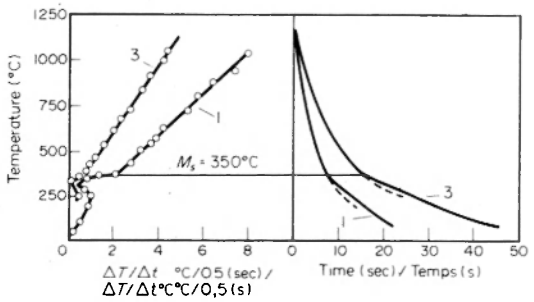

Fig.3 : Direct rate analysis of temperature-time curves (Phillips [7]).

in an approximately linear plot until transformation occurs. At this temperature a marked deviation from linearity is seen (Fig.3).

The differential thermal analysis [7] is considered to be one of the most sensitive methods for recording the temperature for the start of transformation. The temperature is continuously compared with that of a reference specimen. The heat liberated results in a tem-

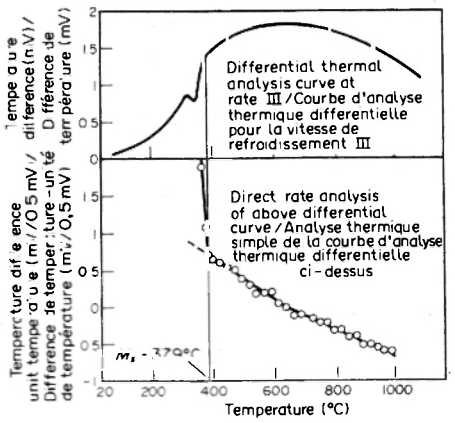

Fig.4 : Derived differential thermal analysis curve (Phillips [7]).

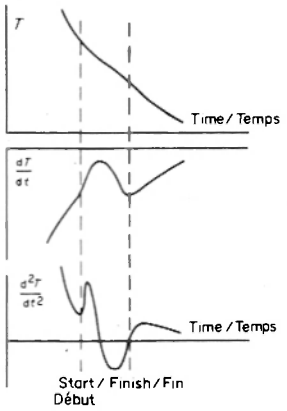

Fig.5 : Thermal analysis of temperature-time cycle. Schematic illustration of the primary curve and the first and second derivatives. The start and finish of the transformation are marked (Nilsson [8]).

perature difference between the test sample and the reference specimen and at the onset of transformation this difference increases remarkably (Fig.4a). The precision can be further improved by applying direct rate analysis to the differential curve. This method is named derived differential thermal analysis. An example is given in Fig.4b indicating a nearly straight line until the M_s temperature is reached. However, according to Phillips [7], the thermal analysis methods seem to lack the sensitivity to locate B_s, B_f and M_f, while the M_s temperature is satisfactorily established.

The cooling programme, recorded on magnetic tape, may also be plotted vs time as T, dT/dt and d^2T/dt^2 as seen in Fig.5 [15].

The temperature-time cycle can also be analysed as follows [16] : The cooling programme is considered from a chosen level Ti in the high temperature range, where the time t is taken to be equal to zero. The rate of heat loss, - dQ/dt, from the sample at temperature T to surroundings at temperature T_o, is approximately proportional to this difference :

$$-\frac{dQ}{dt} = \frac{dT}{dt} \sim T - To$$

By integration :

$$T - To = (Ti - To) \exp(-Bt) \quad (1)$$

Where B is a constant,

Equation (1) gives by logarithmic differentiation :

$$\ln(T - To) = \ln(Ti - To) - Bt \quad (2)$$

$$\frac{b \ln(T - To)}{dt} = -B. \quad (3)$$

The slope of the cooling curve on a logarithmic scale is thus, according to eq. (3) equal to -B, both in the high and low temperature range (above and below the phase transformation). As indicated in Fig.6, the observed slope in the phase transformation range will show a pronounced deviation from the curve described by eq. (3).

In the case of martensite microstructures, the M_s and M_f can be fairly precisely determined by the two methods illustrated in Figs. 5 and 6. Furthermore, when a split transformation occurs involving significant amounts of ferrite sideplates, the B_s can also be measured with fair precision. The problems connected with determining B_f and M_f are inherent in the relatively low amounts of heat liberated at the end of transformation.

For the purpose of comparison of the different techniques, Phillips [7] showed that for fast cooling, thermal analysis gave the most precise transformation temperature. At slow cooling the dilatometric technique appeared

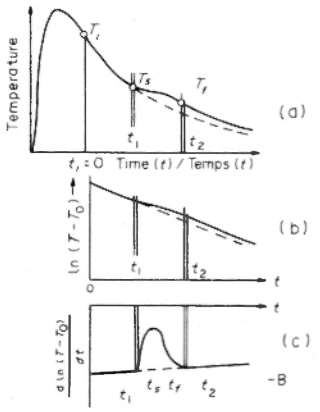

Fig.6 : Example of temperature recording (a) and signal processing (b) and (c) (Christensen and Simonsen [16].

as the most precise method. More recent work in the authors' laboratory indicates that both methods give approximately the same temperatures for cooling times $\Delta t_{8/5}$ in the range from 5 to 30 sec. Slower cooling corresponding to $\Delta t_{8/5}$ longer than 30 sec indicates that dilatometric analysis should be applied.

Thermal analysis of phase transformation occurring in reaustenitized weld metal deposits is discussed in ref. [15a] and ref. [16]. Dilatometric analysis is also frequently used in weld thermal simulation of the high temperature response of reaustenitised weld metal samples [17].

2.2 The real welding situation :

The weld metal transformation, which occurs during cooling from crystallization, may be assessed by the thermo-harpoon technique [18]. The temperature and the first and second derivatives are obtained directly from the thermo-harpoon signal. This method has recently been used for determining transformation temperatures in submerged-arc weld metals [19]. Dilatometric analysis has been applied to in situ examination of the transformation behaviour in the HAZ [11]. This technique, however, does not seem to be fully developed at the present time. A more simple and material saving method is the "implant" procedure [20]. A test bar is inserted into a mild steel plate where thermal analysis of the recorded temperature-time curve may be made using chromel-alumel thermocouples as shown in Fig.7. The thermocouples are positioned where the HAZ of a bead is expected to come. In Fig.7 the thermocouple indexed A measures the temperature while that indexed B is a reference thermocouple (mineral insulated, isolated junction thermocouple encased in stainless steel). The thermocouples are connected so as to measure the temperature T at the cooler point during the cooling stage (index A) and the temperature difference ΔT between the warmer and the cooler point (B-A).

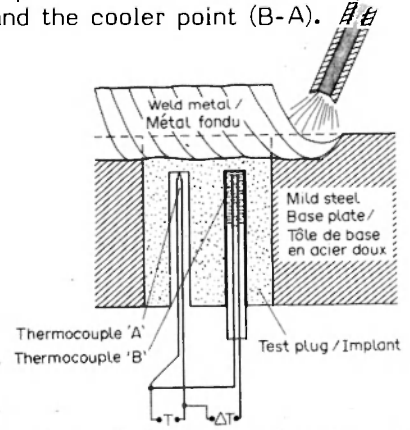

Fig.7 : Thermal analysis set-up for determining the transformation temperature in a real HAZ (Phillips [21]).

Examples from these experiments are given in Fig.8. It is seen that the start of transformation is taken as the point where the temperature difference during cooling starts to diminish rapidly, while the finish of transformation is considered as the point where the deviation from a smooth curve in the transformation discontinuity appears to end. One should note that the thermocouple A, due to its position on the cooler side, first registers any transformation, which in turn cause the temperature difference between A and B to diminish. the method seems to be quite sensitive, M_s and B_s being recorded at values down to 8% and 12% respectively.

3.0 Comparison between simulated and as-welded HAZ transformation behaviour

Several papers have been published on the comparison between simulated and as-welded HAZ microstructures [12,22]. Small variations in the microstructural composition have been reported. These variations are also reflected in the transformation temperatures. From the work by Phillips [21], it emerges that both the martensitic and non-martensitic transformations occur at lower temperatures during simulation than in the actual HAZ. Differences up to 140°C were observed for non-martensitic constituents. Additionally, bainite first appeared at somewhat faster cooling rates in the actual HAZ. This trend was reversed at the slower cooling rates where the fraction of martensite was higher in the actual HAZ. The differences in the transformation temperatures are indicated in Fig.9, showing CCT-diagrams for weld thermal simulation (dilatometry) and the actual welding ("implant" thermal analysis).

The main problem during weld thermal simulation, however, seems to be matching the austenite grain size with that of the coarse-grained zone in a real weldment. According to Dolby and Widgery [23] the peak temperature during simulation at 1210°C matched the austenite grain size in the grain coarsened region of the HAZ, the often used peak temperature of 1350°C giving larger grain size than the as-welded condition. This supports previous findings by Berkhout and van Lent [12]. These differences have among other factors been attributed to different heating rates, the heating rates during simulation being too slow [21,24]. Slower heating rates allow the grain growth inhibiting precipitates to dissolve at a slightly lower temperature, thus increasing the temperature range where grain growth can occur. Differences in grain size will probably also be expected in a steel without grain growth inhibitors. The restraint intensity has also been proposed as an additional explanation of the difference in grain size.

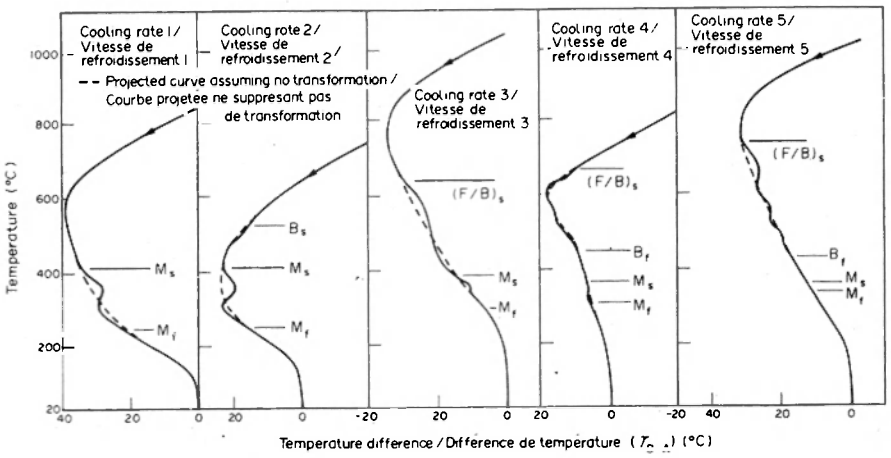

Fig.8 : Examples of thermal analysis curves for different cooling rates from real weldments (decreasing cooling rate to the right) (Phillips [21]).

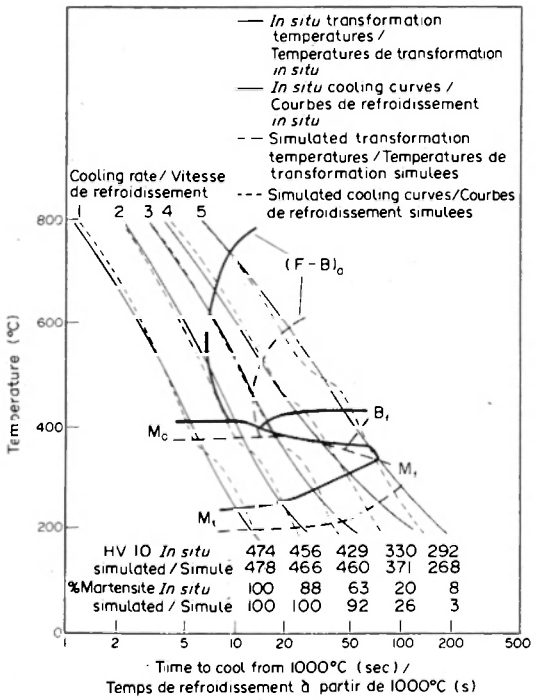

Fig.9 : Comparison of in situ and simulated CCT-diagrams for a C-Mn steel (Phillips [21]).

Furthermore, steep temperature gradients in the real HAZ have also been considered. This latter explanation seems more likely due to the fact that the grain growth occurs from the fusion line toward lower temperatures, as distinct from the simulated condition where the austenite grains can grow in all directions.

In spite of the above mentioned discrepancies, the weld thermal simulation is a frequently used method for assessing the transformation behaviour in heat affected zones.

4. Closing remarks

Several years ago empirical equations were introduced to describe the start and finish of the martensitic and bainitic transformations (summarized in ref. [25]) :

$$Bs = 830 - 270(\%C) - 90(\%Mn) - 37(\%Ni) - 70(\%Cr) - 83(\%Mo) \quad (4)$$

$$Bf = Bs - 120 \quad (5)$$

$$Ms = 561 - 474(\%C) - 33(\%Mn) - 17(\%Ni) - 17(\%Cr) - 21(\%Mo) \quad (6)$$

$$Mf = Ms - 215 \quad (7)$$

Bs, Bf, Ms and Mf are expressed in °C

Similar equctions have also been proposed for the A1 and A3 temperatures. However, these formulae are probably not valid for other steel compositions than those from which they were developed. In spite of the uncertainties involved, mathematical calculation of transformation diagrams has been further developed [26,27]. It has also become possible by computer programs to predict the microstructures expected in the HAZ of weldments [28]. Before applying these mathematical calculations various parameters such as the thermal efficiency factor for the welding method used and the thermal diffusivity (or conductivity) of the actual steel composition must be known rather precisely. Moreover, the situation is further complicated in the case of a multipass weldment. Attempts have also been made to simulate this condition [29].

It will be noted that the equipment used for measurement of transformation behaviour has not been discussed. Such information is given in detail in the references. Clearly there

has been considerable improvement in that particular area throughout the years. Another topic which seems attractive is the development of microscopes for high temperature services, as for instance the microscope applied to the observation of grain boundary liquation in the partially melted region of the HAZ [30]. The application of the microscope to transformation behaviour (optical dilatometry) has recently been discussed by Ruge et al. [31]. These new developments and improvement should stimulate further research ; however, thermal analysis and dilatometry will probably remain as useful methods.

References

1. **R.C. Cochrane** : "Weld metal microstructure and terminology. Document of the IIW II-A-444-78.

2. **D.J. Abson, R.E. Dolby** : "A scheme for the quantitative description of ferritic weld metal microstructure.

3. **R.J. Pargeter** : "Quantification of weld metal microstructure". Document of the IIW IX-J-37-80.

4. **Japanese work** : "Classification of microstructures in low C-low alloy steel weld metal and terminology". Document of the IIW IX-1282-83(II-A-597-83).

5. **P.L. Harrison, M.N. Watson, R.A. Farrar** : "Continuous cooling transformation (CCT) diagrams for niobium bearing HSLA weld metals". Schweissmitteilungen, Oerlikon, 100 pp. 11-24, Nov. 1982.

6. **M. Inagaki, M. Uda, T. Wada** : "A new apparatus for determining SH-CCT diagram for welding and its application to high strength steels". Document of the IIW IX-438-65.

7. **R.H. Phillips** : "Improved techniques for determining transformation temperatures during simulated welding conditions". Br. Weld. J., pp. 547-552, 1968.

8. **K. Nilson** : "Hardenability of carbon-manganese steels in welding". Jernkont, Ann., Vol.153, pp. 121-137, 1969.

9. **A Graef** : "Determination of the transformation behaviour in steels during rapid continuous cooling". Ibid., pp. 139-143 (in Swedish).

10. **O. Saetre** : Met. Eng. Thesis. The Norwegian Inst. of Technology, 1973 (in Norwegian).

11. **W. Hofmann, F. Burat** : "Immediate recording of continuous TTT-diagrams during welding and studies on cold cracking". Document of the IIW IX-318-62.

12. **C.S. Berkhout, P.H. van Lent** : Use of high temperature cooling diagrams during welding of high strength steel. Schweissen und Schneiden, Vol. 20, pp. 256-260, 1968.

13. **A. Constant, G. Murry** : Soudage et Techniques Connexes, Vol. 17, pp. 405, 1963.

14. **E.F. Nippes, W.F. Savage** : "Development of specimen simulating weld heat-affected zones". Weld. J., Vol. 28, Res. Suppl., pp. 534s-545s, 1949.

15. **SINTEF** : Project on transformational behaviour weld metal. K. Pedersen, N. Christensen : Document of the IIW II-A-446-78 ; M. Syverud, T. Simonsen, N. Christenses : Document of the IIW II-A-463-79 ; T. Simonsen, N. Christensen : Document of the IIW II-A-470-79.

16. **N. Christensen, T. Simonsen** : "Transformation behaviour of weld metal". Scand. J. Met., Vol. 10, pp. 147-156, 1981. Document of the IIW II-A-520-80.

17. **P.L. Harrison, R.A. Farrar** : "Influence of oxygen-rich inclusions on the $\gamma \rightarrow \alpha$ phase transformation in high-strength low-alloy (HSLA) steel weld metals". J. Mat. Sci., Vol.16, pp. 2218-2226, 1981.

18. **C. Pedder** : "Harpoon thermocouples". Weld. Inst. Res. Bull. Vol. 14, pp. 333-334, 1973.

19. **D.J. Abson, R.E. Dolby, P.H.M. Hart** : "The role of non-metallic inclusions in ferrite nucleation in carbon steel weld metals". Proc. of the Conf. on Trends in Steels and Consumables for Welding, 1978, Paper 25, pp. 75-101. The Welding Institute, Abington, Cambridge.

20. **H. Granjon** : "The implants method for studying the weldability of high strength steel". Met. Constr. Br. Weld. J., pp. 509-515, 1969.

21. **R.H. Phillips** : "In situ determination of transformation temperatures in the weld heat-affected zone". Weld. J., Res. Suppl., 12s-18s, 1983.

22. **C.F. Berkhout** : "A comparison of the microstructures in the simulated and weld HAZ". Thermal Simulators for Research and Problem Solving, Seminar Handbook, London, 27th April, 1972, Paper 4, pp.21-24, The Welding Institute, Abington, Cambridge.

23. **R.E. Dolby, D.J. Widgery** : "The simulation of HAZ microstructures". Weld. Inst. Report M53/70, 1970.